RC22445 (W0205-123) May 15, 2002
Materials Science

IBM Research Report

IN SITU MONITORING OF THIN FILM REACTIONS DURING RAPID THERMAL ANNEALING: NICKEL SILICIDE FORMATION

C. Lavoie, R. Purtell [1] , C. Coïa [2] , C. Detavernier, P. Desjardins [2] , J. Jordan-Sweet, C. Cabral, Jr.,F.M. d'Heurle, J.M.E. Harper.

IBM T.J. Watson Research Center
Yorktown Heights, New York 10598, USA

[1] IBM Microelectronics Division
East Fishkill Facility, Hopewell Junction, NY 12533, USA

[2] Département de génie physique
École Polytechnique de Montréal, Québec, Canada

Research Division
Almaden - Austin - Beijing - Delhi - Haifa - India - T. J. Watson - Tokyo - Zurich

IN SITU MONITORING OF THIN FILM REACTIONS DURING RAPID THERMAL ANNEALING: NICKEL SILICIDE FORMATION

C. Lavoie, R. Purtell[1], C. Coïa[2], C. Detavernier, P. Desjardins[2], J. Jordan-Sweet, C. Cabral, Jr., F.M. d'Heurle, J.M.E. Harper.

IBM T.J. Watson Research Center, Yorktown Heights, New York 10598, USA
[1] IBM Microelectronics Division, East Fishkill Facility, Hopewell Junction, NY 12533, USA
[2] Département de génie physique, École Polytechnique de Montréal, Québec, Canada

ABSTRACT

Using *in situ* characterization during rapid thermal annealing in conjunction with transmission electron microscopy, we demonstrate that multiple metal rich phases are present in the Ni-Si system when reacting a thin Ni film with an underlying Si substrate. The formation temperatures for the metal rich phases highly depend on dopant type but are relatively insensitive to surface preparation. We also show that a serious limitation for NiSi implementation in devices is the low morphological stability of the film, which degrades before the monosilicide transforms to the high resistivity $NiSi_2$ phase. The nucleation of this latest phase is not desired in devices not only because the resistivity of the phase is larger but also because its formation requires more consumption of the Si substrate which is limited in state-of-the-art devices. The nucleation occurs at lower temperature in thicker films because of the higher area density of nucleation sites. We also find that the nucleation of $NiSi_2$ is very dependent on the temperature ramp rate as the morphological degradation of the film competes with the nucleation processes and retards the phase formation.

INTRODUCTION

The demand for more flexibility in semiconductor device design has stimulated considerable effort for the development of materials structures with adjustable properties. Such structures, for example metal silicides in CMOS circuits, are often obtained through precise engineering of rapid thermal processing. It is therefore critical to develop the ability to characterize the effects of annealing conditions on final materials properties.

For current microelectronic devices, the constant decrease in critical dimensions regularly leads to some practical limits in the properties of the material used. As a consequence, it becomes essential to optimize current materials either through variations in processing conditions to tailor the layer microstructure or through changes in materials composition (alloying) or even by introducing completely new materials to reach the desired properties. This optimization of materials and processing conditions is becoming extremely expensive to perform on integrated wafers as device development is moving to 300 mm wafers, hence the need to achieve a process and material optimization that stays ahead of implementation.

In this work, we present our development of simultaneous measurements of film properties during annealing at rates up to 50 °C/s. We use a combination of *in situ* monitoring techniques to follow changes in phases, texture, resistivity and surface roughness as reactions occur in thin

film systems. The use of high intensity x-ray beams available at synchrotron facilities and fast linear detector arrays allows for time resolved diffraction measurements and phase identification during temperature excursions at high ramp rates. Sample resistance is simultaneously measured using a square four-point probe geometry, while the surface roughness information is acquired by following the evolution of scattered light intensity from a laser source [1-4].

Using our *in situ* technique, in conjunction with transmission electron microscopy (TEM) measurements, we present the characterization and phase identification during the reaction of a Ni film with a Si substrate. As the production of devices moves towards thin silicon-on-insulator (SOI) substrates, this materials system becomes critically important for the formation of silicide contacts to CMOS devices since it permits a reduction of Si consumption from the substrate compared to the formation of cobalt disilicide contacts currently used in advanced devices. The phase of interest for microelectronics applications, nickel monosilicide (NiSi), has a resistivity of about 13-14 μΩ cm in thin films while that of $CoSi_2$ is about 18 μΩ cm. This allows for a reduction in the silicide thickness for the same sheet resistance. Moreover, since the desired Ni silicide phase is the monosilicide (vs. disilicide for the Co-Si system), the density of Si atoms in this phase is lower than that of $CoSi_2$ and the consumption of Si from the substrate is thus further reduced. Typical savings on Si consumption for obtaining the same sheet resistance are around 30%.

In moving from the current $CoSi_2$ to the new NiSi contacts, multiple challenges are to be expected. The Ni-Si phase diagram is much more complex than that for Co-Si as shown in Fig. 1. While only three phases can be present at room temperature in the Co-Si system (Co_2Si, CoSi and $CoSi_2$), one can count up to eleven phases in the Ni-Si diagram, six of which being stable at room temperature (Ni_3Si, $Ni_{31}Si_{12}$, Ni_2Si, Ni_3Si_2, NiSi and $NiSi_2$) [5]. This considerably increases the complexity of the phase formation sequence and its possible dependence on processing parameters and substrate variations (dopant type and concentration, cleaning conditions, substrate type). In spite of the increased complexity, traditional studies of the interaction of Ni films (about 100 nm thick) with Si substrates carried out using isothermal anneals followed by *ex situ* characterization have revealed only the sequential formation of Ni_2Si, NiSi and $NiSi_2$, remarkably similar to the Co-Si reaction [6]. We show here that for samples prepared by standard device manufacturing processes and for film thicknesses relevant to the state of the art CMOS technology, multiple metal rich phases appear during rapid thermal anneals at rates and temperatures typical of manufacturing processing conditions.

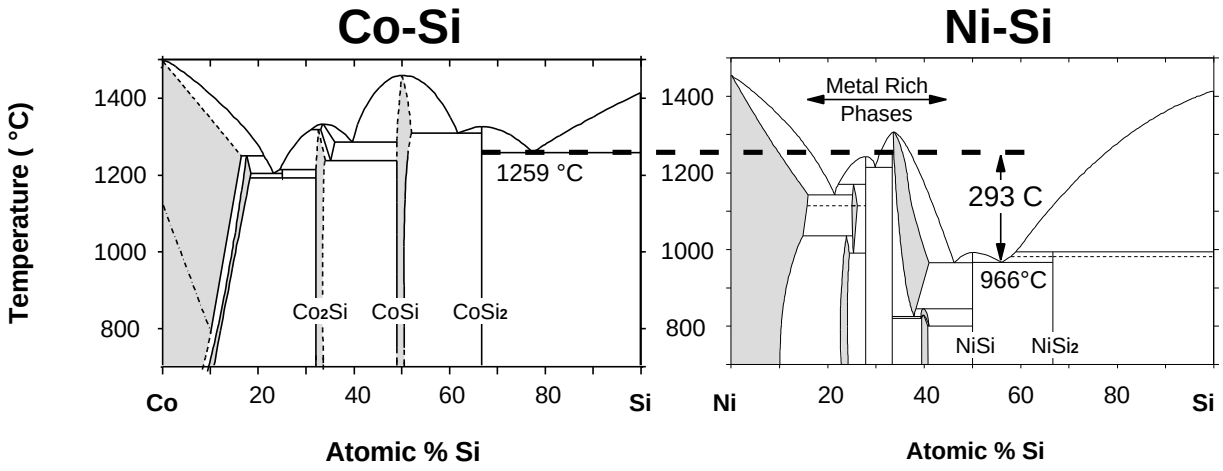

Fig. 1. Comparison of phase diagrams for Co-Si and Ni-Si. Note the increased complexity in number of stable phases at room temperature and the lower temperature for melting.

The other important challenge to mention is that the nickel monosilicide phase is expected to be more unstable morphologically than its cobalt disilicide counterpart. The formation temperature of NiSi is reported as being at least 75 °C lower than CoSi showing a higher diffusivity for Ni atoms over Co atoms [7]. The Ni atoms are also expected to be more mobile from comparing the melting points of the materials. As shown in Fig.1, the eutectic melting on the Si rich side of NiSi (966 °C) is nearly 300 °C lower than for $CoSi_2$ (1259 °C). Note that if one uses directly the melting temperatures of the phases ($CoSi_2$: 1326 °C, NiSi: 992 °C) instead of the eutectic temperatures, the difference is even larger. For a given annealing temperature, the NiSi film will therefore be closer to the melting temperature and become more likely to agglomerate. Moreover, because of its lower resistivity, the problem will be amplified since the silicide layer is thinner for a given sheet resistance.

EXPERIMENT

Ni films, 7.5 to 15 nm thick, were deposited onto p- and n-type silicon on insulator (SOI), Si(100) or poly-Si substrates by magnetron sputter deposition. The implantation doses were 5E15 cm^{-2} at 12 keV for phosphorous atoms and 3.5E15 cm^{-2} at 8 keV for boron atoms. Standard substrate cleaning procedure were performed in which the final substrate preparation always included a dilute HF acid etch. Some samples were blown dry without rinsing and loaded directly in a UHV sputtering system while others were rinsed in deionized water after the HF etch. Samples were kept in dry boxes (nitrogen) before measurements and anneals. In order to establish if surface oxidation had any significant effect on the reaction kinetics, some of the Ni films were capped *in situ* with 20 nm of TiN (without air exposure). The phase formation sequence was found to be essentially identical in capped and uncapped films even after air-exposure for several months.

The annealing experiments were performed at the National Synchrotron Light Source (NSLS) X20C beamline at Brookhaven National Laboratory (NY, USA) where we followed *in situ* the formation of different phases via the development of their characteristic diffraction patterns [1-4]. The samples consisted of 1.5x1.5 cm^2 squares cut from Si wafers. After multiple evacuations of the vacuum chamber, purified N_2 or He with oxygen contamination far below the part-per-trillion level (ppt) was flowed during the high temperature excursion. In the current experiments, samples were annealed at a rate of 3 °C/s. The temperature measurements were calibrated using metal-silicon eutectics and are precise to ± 3 °C.

For the x-ray diffraction (XRD) part of this experiment, we selected an energy of 6.9 to 7 keV (λ = 0.177 to 0.180 nm) using a multilayer monochromator. For most of the measurements shown here, the x-ray wavelength was 0.1776 nm as determined from the Si(220) peak position. The monochromator provides an energy resolution of 1.5% that translates into an x-ray flux greater than 10^{13} photons/s. This corresponds to a gain of four orders of magnitude over a state of the art rotating anode XRD system. The combination of the high x-ray photon flux with a linear position-sensitive detector allows both fast data acquisition during rapid thermal anneals (RTA) and measurement of very thin films. In the current configuration, a diffraction curve (covering a range of 2θ angles of up to 14°) from a ~10 nm metal film can be acquired in less than 100 ms. Unless specified otherwise, the x-ray beam was incident at an angle of 27° from the plane of the sample. This incidence angle was selected since it allows to maintain near Bragg-Brentano geometry for characteristic x-ray lines from all important phases in the Ni-Si system within the 2θ window of the linear detector.

The experimental apparatus is designed [4] so that one can simultaneously monitor both the film resistance using a four-point probe setup and the surface roughness via the elastic scattering of monochromatic light. Roughness measurements [8] are made using a HeNe laser light with a wavelength of 633 nm, at an incident angle of 65° and scattered angles of -20° and 52° (with two detectors) providing information on lateral length scales of about 0.5 μm and 5 μm, respectively. The detection of low intensity scattered light during high temperature anneals requires optical filtering and lock-in detection in order to eliminate intense black body radiation from the sample.

Selected samples were annealed and "quenched" in the various phases observed with the in situ measurements and were analyzed using transmission electron microscopy (TEM). Specimens were prepared in cross-section with [110] surface normals and in plan-view using conventional mechanical polishing followed by room-temperature low-angle (4°) Ar ion milling at 5 keV in a Gatan precision ion polishing system (PIPS). The ion energy was progressively reduced to 3.5 keV during the final stages of thinning in order to minimize sample damage and to obtain samples with relatively even thickness distributions. Images were recorded at 300 kV on a Philips CM30 microscope.

RESULTS

Phase formation sequence and identification of metal rich phases.

The results from the reaction of a 15 nm film of Ni with p-doped polycrystalline Si are displayed in Fig. 2 as measured using time resolved XRD during an anneal at 3 °C/s in a purified nitrogen ambient. Two peaks are present at low temperature in the selected 2θ window (50 to 60 degrees). The first one near 52° is the (111) diffraction line of Ni. The second, slightly above 55°, is the (220) diffraction line from the poly-Si substrate. As the temperature increases to 300 °C, the Ni peak starts to decrease in intensity while another appears at about the same position as the Si(220). Considering the metal rich phases alone, this peak position matches the (350) spacing of Ni_3Si_2 [9]. When the temperature reaches 400 °C, the peak from the metal rich phase has disappeared and two low intensity peaks from the monosilicide phase can be observed: NiSi(103) just below 60° and NiSi(112) at about 53°. Note that there is a clear decrease of the Si(220) peak intensity: a consequence of Si consumption during Ni silicide formation. At about 800 °C, the two weak NiSi peaks disappear as the $NiSi_2$(220) peak intensity increases. This phase forms relatively quickly and is stable over a temperature range of less than 200 °C as both the poly-Si and $NiSi_2$ intensities decrease drastically upon reaching the eutectic melting temperature of 966 °C. While the decrease in $NiSi_2$ intensity is a direct consequence of melting, the disappearance of the poly-Si peak is more surprising and could be the result of texturing in the poly-Si layer in the presence of the liquid.

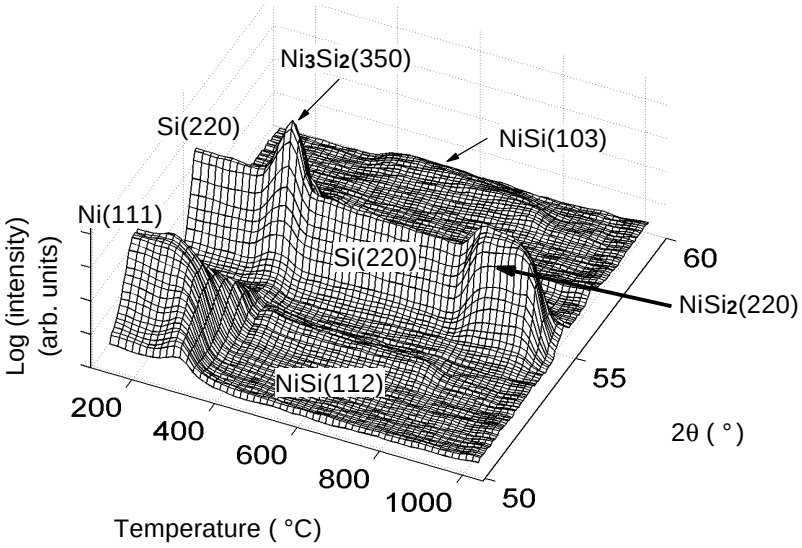

Fig. 2. 3D rendering of the *in situ* x-ray diffraction measurements during annealing of a 15 nm Ni film deposited on p-doped poly-Si. (3 °C/s)

The x-ray data is replotted in a top view (Fig.3b), together with the simultaneous resistance and light scattering data (Fig. 3a). In this way, it becomes clear that the high photon flux available from the synchrotron ring allows the detection of significant modifications to the Ni layer starting just above 200 °C. Furthermore, at least three metal rich crystalline Ni-Si phases are detected. The x-ray intensity in Fig. 3b is presented both as gray logarithmic scale (white is high intensity) and as intensity contours. The peak identification is difficult because of the large number of phases over a narrow temperature range and because of the presence of the poly-Si(220) peak which overlaps many peaks from the metal rich phases. The peak overlap is more important here because of the lower resolution of the selected monochromator (1.5%). Thermal expansion and strain relaxation during annealing also complicate the phase identification.

Although, the phase formation sequence at low temperature is relatively complex and multiple anneals to specific temperatures are needed to identify the phases using *ex situ* techniques (as discussed below), one can already learn considerably from this narrow *in situ* 2θ x-ray diffraction window. Starting around 200 °C, the Ni (111) peak already shifts towards larger 2θ values (lower part of the Ni peak on Fig. 3b). This shift could be the result of some strain relief related to grain growth combined with the possible appearance of some Ni_3Si. Because this phase has a high symmetry (cubic) only one diffraction line is present in the current 2θ window at ~52.2°. From 250 °C to 300 °C the increases in intensity on each side of the Ni peak as well as the appearance of the peak below the Si(220) correspond well to the 024 and 122 (49.9° and 51.1°), 115 (53.3°) and 205 (56.6°) diffraction lines of the $Ni_{31}Si_{12}$ phase [10]. At about 340 °C, the clear peak at 53.0° may be the (301) and (121) lines (same d spacing) of orthorhombic Ni_2Si, while the extra shoulder at about 57° corresponds well to the (002) line of the same phase [11] (will be referred to only as Ni_2Si below). The very intense peak seen around 370 °C at about 55.6° can be indexed as Ni_3Si_2 {(350) line at 55.4°}[9]. From 390 °C to 420 °C, the peak at about 53.5° that remains up to 750 °C corresponds to NiSi (210). It could also be indexed as the (211) line of Ni_2Si for the lower temperatures.

The simultaneous measurements of resistivity and scattered light shown in Fig. 3a are useful in revealing film transformations that may not be visible by x-ray diffraction or not present in the selected 2θ window. The resistance

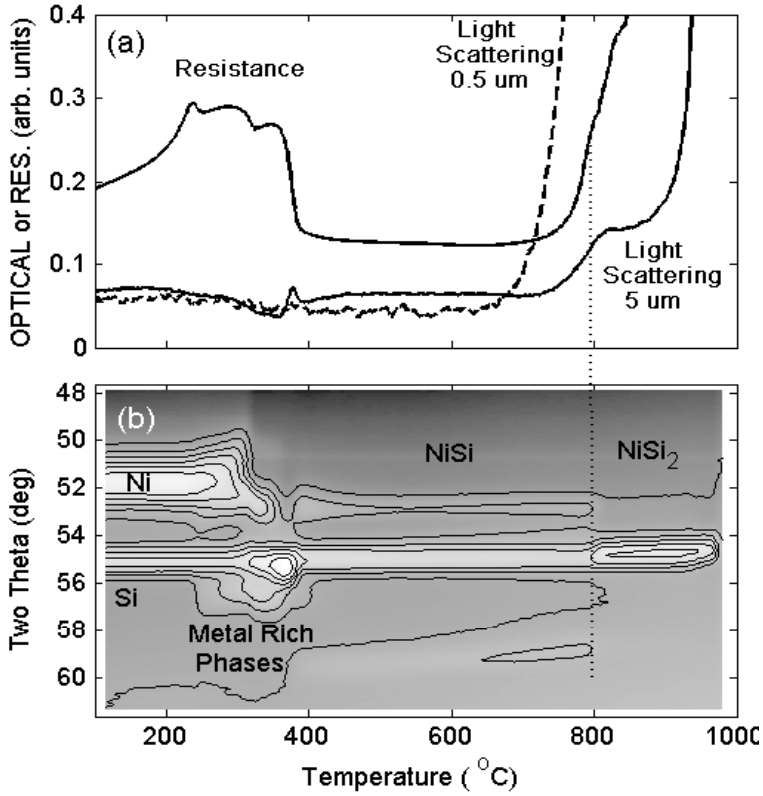

Fig. 3 (a) Resistance and light scattering from 0.5 and 5 μm length scales together with (b) x-ray diffraction measurements performed *in situ* during annealing (3 °C/s) of a 15 nm Ni film deposited on p-doped poly-Si.

is particularly sensitive to the formation of the metal rich phases. As expected from the temperature dependence of the resistivity in metal films, the resistance first increases linearly with temperature for the lower temperatures. Just below 250 °C, corresponding to the appearance of the slight shoulder in the Ni(111) peak, the resistance starts to increase more rapidly. As the temperature increases further, the resistance then goes through three local maxima pointing to the complexity of the formation sequence before the formation of the low resistivity NiSi. The resistance then remains low for a temperature window of about 400 °C. At higher temperature (starting < 800 °C), the resistance increases drastically as the film agglomerates, the higher resistivity $NiSi_2$ phase forms and the film finally melts.

During the formation sequence, the light scattering signals also show very distinct signatures. The shorter length scale light scattering signal (0.5 µm) remains low through the formation of all Ni rich and monosilicide phases, up to a temperature higher than 600 °C. In contrast, the 5 µm signal changes significantly slightly below 400 °C. On this length scale, the signal first goes through a maximum that corresponds exactly to the sharp decrease in resistance and then stabilizes at a higher intensity. This increase could result from different optical constants for the phases. It could also be correlated with either surface pits appearing as NiSi starts to form or could also be related to the reported low temperature formation of $NiSi_2$ inverted pyramids [12]. The large increase in surface roughness at high temperature begins below 700 °C for the 0.5 µm signal and at about 750 °C for the 5 µm one. For both length scales, the roughening clearly starts before the transformation to the high resistivity disilicide as observed by XRD. This suggests that for the processing conditions used here, the agglomeration of the thin NiSi film precedes the disilicide formation and should be the limiting factor for integration of nickel silicide in microelectronics.

The influence of dopant type on the formation of metal rich silicide phases is presented in Fig. 4 using the x-ray diffraction curves for p and n doped SOI substrates (Si on insulator). Without the presence of the poly-Si(220) peak, the peaks from the metal rich phases are better defined. One of the phase identifications suggested above is indicated directly on the figure. Both the temperature of formation for the phases and the phase sequence clearly depend on dopant type. For example, in this possible phase identification, the peak that represents the orthorhombic Ni_3Si_2

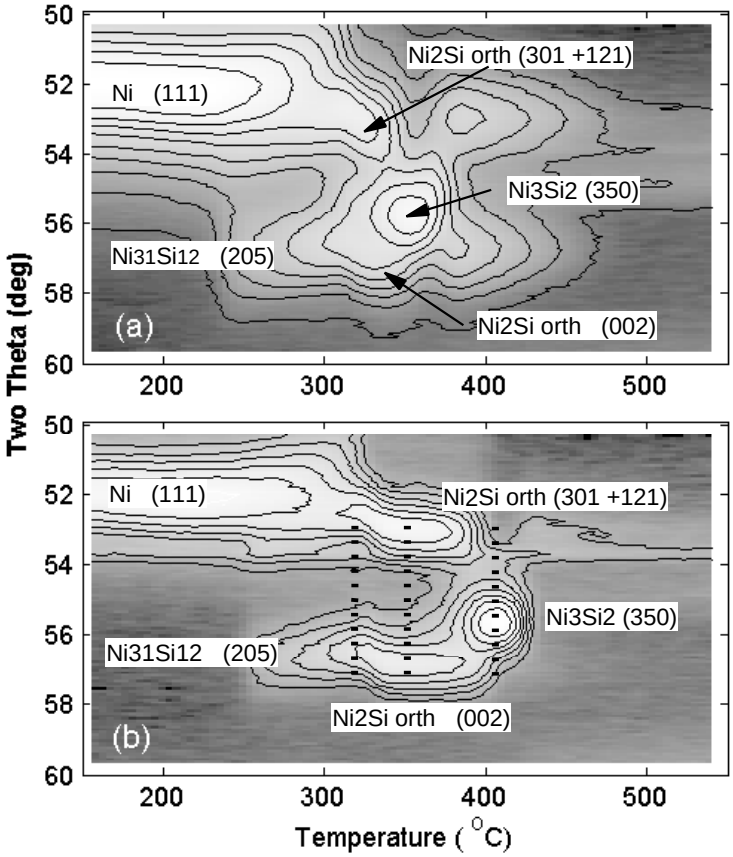

Fig. 4 In situ x-ray diffraction measurement during annealing of a 15 nm Ni film deposited on (a) p-doped and (b) n-doped SOI substrate.

appears around 350 °C for p-doped SOI while it appears at about 400 °C for n-doped SOI substrates. A 50°C difference at these low temperatures and relatively low ramp rates (3 °C/s) shows the influence of the dopant on the diffusion kinetics.

To gather more information on the metal rich phases, selected anneals at different temperatures were performed in each of the phases identified with vertical dotted lines in Fig. 4b. The current characterization system allows for the determination of annealing temperatures that correspond precisely to the phases observed. The monitoring of x-ray intensity during cooling also insures that the desired crystalline phase has been "quenched in" and that no significant modification to the crystal structure occurred on cooling. The selected temperatures are given in Table 1. Although the sequence is relatively similar at low temperatures for the n and p doped substrates we first selected the n doped substrate since the phases have a larger temperature range of existence and are thus better defined.

Cross-sectional TEM bright-field images from samples annealed at 320, 350, and 408°C are presented in Fig. 5. The layers appear fully-dense with no evidence of either inter- or intragrain porosity. The images also indicate that the layers are uniform in thickness at all annealing temperatures, with no indication of the formation of a multilayered system as expected for competitive growth of multiple phases. Most grains extend across the thickness of the layer in all samples. The silicide layer thickness increases slightly from sample B to C, and by a factor 1.18 from C to D. Although the roughness of the layers introduces some uncertainty in the thickness, this result is in agreement with the predicted 15% expansion between orthorhombic Ni_2Si and the Ni_3Si_2.

n-doped SAMPLE	A	B	C	D
Anneal Temperature	As deposited	320 C	350 C	408C
Phase	Ni	Ni31 Si12	Ni2Si orth	Ni3Si2
Average Layer thickness	16 nm	20 nm	22 nm	26 nm
Average Grain Size	12 nm	28 nm	28 nm	28 nm

Table 1. List of individual anneals for a Ni film on n-doped SOI substrate. The anneal temperatures, the expected crystalline phases from *in situ* diffraction, the metal/silicide layer thicknesses and the grains sizes are listed.

Fig. 6 shows plan-view TEM images, obtained in bright-field conditions, together with selected-area electron diffraction (SAED) patterns from the same samples as in Fig. 5 and the as deposited sample. The layers are fully dense in agreement with the cross-sectional TEM images shown above. Upon annealing, the grains grow in the in-plane direction from an average dimension of ~12 nm in the as-deposited sample to ~28 nm at 320 °C. Further annealing does not change the grain size significantly. For each SAED pattern the very bright spots are attributed to diffraction from the single-crystal Si substrate while the smaller spots positioned in rings represent diffraction from the polycrystalline metal silicide film. The smaller spots in the diffraction rings are randomly positioned along the ring indicating no in-plane texture. For the Ni film, because the grains are much smaller, the diffraction rings are more uniform.

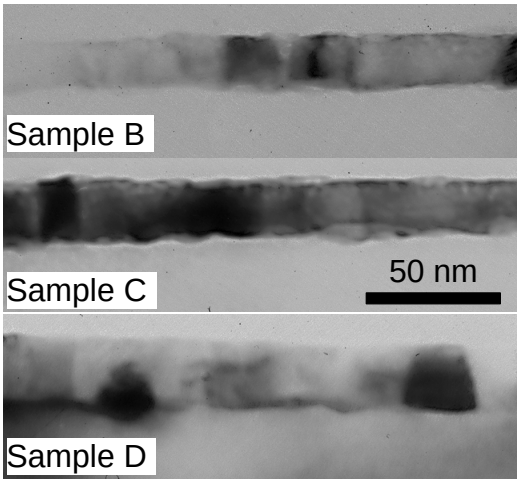

Fig.5. Cross section TEM images of samples B, C and D, annealed at 320 °C, 350 °C and 408 °C.

Although the detailed analysis of the ring position is not presented here, the following conclusions were drawn. Rings observed for sample A can all be associated with fcc-Ni. For the three other samples, the density of rings is very large and their positions clearly change supporting the presence of multiple low symmetry phases that succeed each other as the temperature is increased. However, the number of possible rings for each of the phases is so large that none of the electron diffraction patterns can be assigned unambiguously to a single phase. Considering the error in the measurement, most rings observed in sample B and C

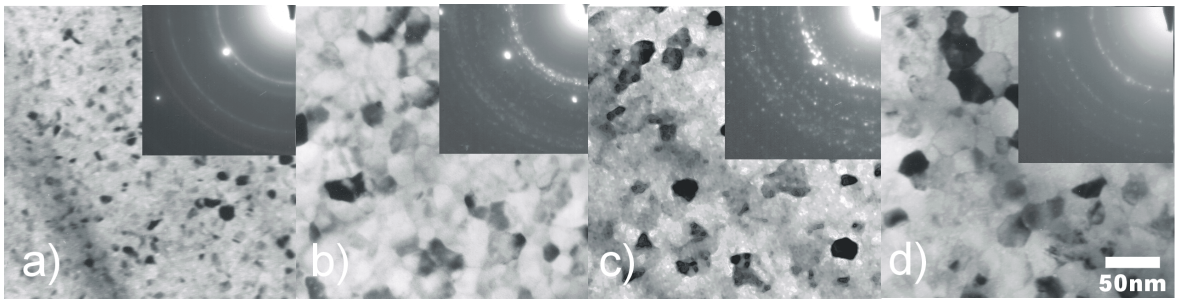

Fig.6. Plan view TEM images and corresponding SAED patterns of samples A, B, C and D as described in table 1.

overlap with rings of the $Ni_{31}Si_{12}$, the Ni_2Si and the Ni_3Si_2. Note this last phase has not been very well characterized and that the expected intensities for d spacings below 1.7 ? are not available in the literature. Certain rings only match either of the first two phases. From the most inner rings, evidence is that from sample B to C the phase would be changing from $Ni_{31}Si_{12}$ and the Ni_2Si. Most of the less dense rings of sample D could match the Ni_3Si_2 phase (for the higher d spacings where data is available) as expected from the *in situ* x-ray measurement. However, the density of possible peaks from the other two phases combined with the error in the measurement prevents us from reaching an unambiguous identification of the phases. To reach this point, further TEM analysis and high resolution triple axis x-ray diffraction are needed.

Morphological stability of NiSi: effect of film thickness and annealing ramp rate

The problem of morphological stability in thin NiSi films is addressed in Fig. 7. Films of Ni with different thicknesses deposited on Si(100) substrates were annealed at 3 °C/s in a purified nitrogen atmosphere. In Fig. 7a, the scattered light from 0.5 μm length scales is displayed for three Ni thicknesses (7.5 nm, 10 nm and 15 nm). In Fig. 7b, the simultaneous x-ray diffraction is shown for the 15 nm thick sample. The disappearance of the three NiSi peaks at about 800 °C corresponds to the formation of $NiSi_2$. In the case of Si(100) substrate, the $NiSi_2$(220) peak is not observed in this geometry since the film becomes epitaxial with the substrate. All three light scattering signals show a two step increase in intensity. Looking at the 15 nm thick sample, it is clear that the second increase corresponds well to the $NiSi_2$ formation. The first increase corresponds to the agglomeration of the monosilicide film. As expected from surface energy arguments, the thinner NiSi film agglomerates at lower temperature. It is also interesting that the second increase in the light scattering moves to higher temperatures for thinner films. This increase in the formation temperature of the $NiSi_2$ was also observed with the simultaneous x-ray measurements (not shown here). An increase in formation temperature for thinner films is consistent with a nucleation controlled reaction: as the NiSi film is thinner, the number of

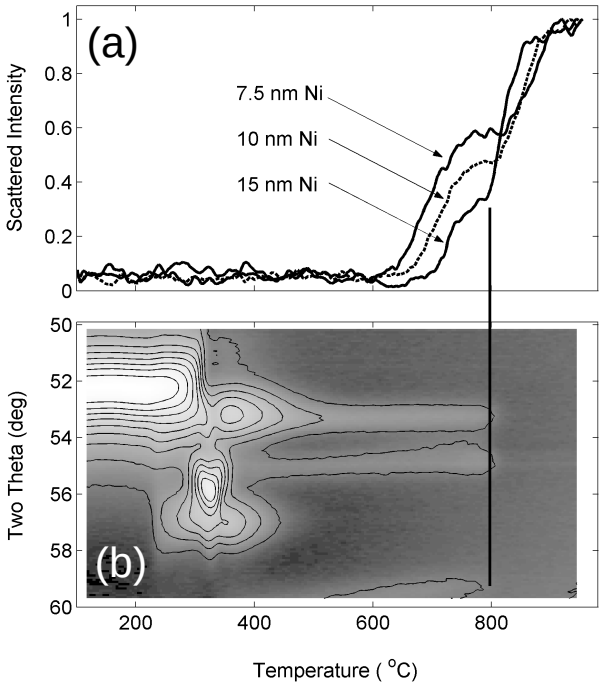

Fig.7 (a) Elastic light scattering at a length scale of 0.5μm performed in situ during three anneals of Ni films of thickness 7.5, 10 and 15 nm deposited on undoped Si(100). (b) Simultaneous x-ray diffraction for the 15 nm film. (3 °C/s)

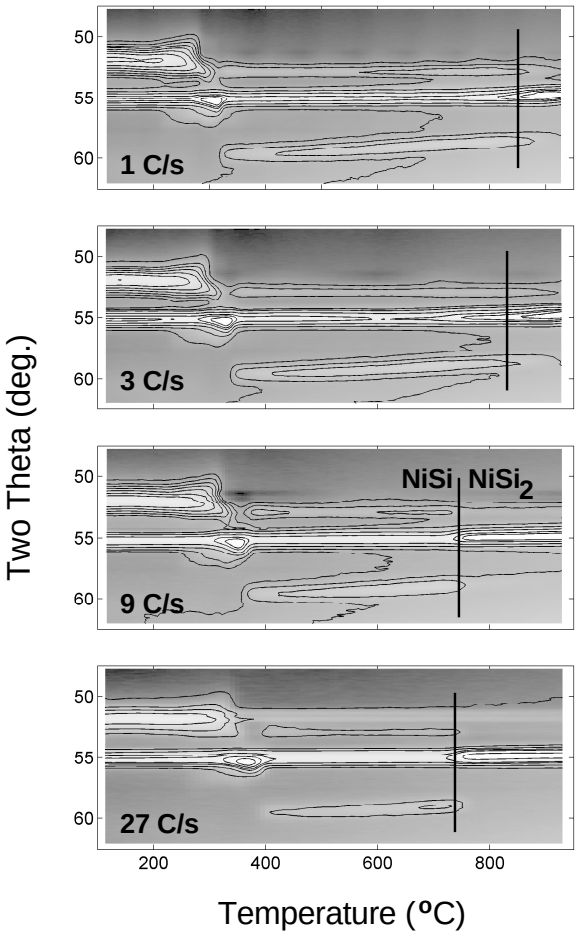

Fig.8 x-ray diffraction measurements during anneal of a 10 nm film deposited on poly-Si. The temperature ramp rate is changed from 1 to 27 C/s. The full line that shifts to lower temperature as the ramp rate increases represent the formation of $NiSi_2$.

necleation sites per unit area decreases and the temperature needed for transformation increases. Also, if the NiSi film forms individual islands before $NiSi_2$ formation, a nucleation center then only lead to the transformation of the island in which it occurred. In order to get any significant fraction of $NiSi_2$, the density of nucleation centers need to increase drastically. This can only occur at higher temperature and lead to a significant increase in formation temperature [13, 14].

The effect of ramp rate on the phase formation sequence for a 10 nm Ni film deposited on poly-Si is presented in Fig. 8. The disappearance of the Ni (111) peak followed by the formation of Ni_2Si and NiSi all behave similarly as the formation temperatures increase with increasing ramp rates as is expected for these types of study. More surprisingly, the temperature at which the $NiSi_2$ forms decreases as the temperature ramp rate is increased. For the lowest temperature ramp rate studied, $NiSi_2$ forms at about 850 °C while its formation temperature is reduced to about 750 °C for the fastest ramp rate. Comparison with resistance and light scattering data (not shown) clearly points to a delay in agglomeration temperature as the ramp rate is increased.

DISCUSSION

Phase formation sequence

Since Co and Ni show so many similarities, in the past when studying their reactions with Si, it was not surprising to find the same sequence of phase formation: dimetal silicide, monosilicide

and disilicide [6,15]. A minor distinction between the two sets is that CoSi has the cubic structure of FeSi, whereas NiSi has the orthorhombic structure of MnP [16-17]. The other two sets of phases have identical structures and the disilicides, both cubic, have nearly the same lattice parameters. The results presented here indicate that the Co-Si and Ni-Si reactions are not as similar as was believed up to now. The phase identification performed here supports the presence of $Ni_{31}Si_{12}$ and Ni_3Si_2 phases. These new findings in the Ni-Si system are undoubtedly a consequence of the more complex phase diagram. However, earlier results obtained with typically thicker films did not show these differences. The first possible origin of the apparent discrepancy with earlier measurements is the power and resolution of the current characterization system. The large gain in intensity (10,000) provides increased signal to noise ratio and allows not only to measure smaller intensities but mainly gives unprecedented temperature resolution as an x-ray diffraction spectrum can be taken every degree C during anneals. It also gives us the ability to quench in a specific phase in a very narrow temperature range. For example, from Fig.4b, the temperature region over which the $Ni_{31}Si_{12}$ peak is not obscured by the Ni peak or already transforming to the Ni_2Si is very narrow, less than 20 °C. This suggests first that obtaining a sample that would contain mainly $Ni_{31}Si_{12}$ is relatively difficult because once it is formed it very rapidly changes to the Ni_2Si. With the current system, even if such a phase can be isolated relatively easily, TEM results show that more than one phase were present in each sample. Other temperature regions over which peaks are present were also very narrow. However, taking into account the amount of work already performed on the Ni-Si system, we find it unlikely that these phases would have been missed entirely.

One could also imagine, as in the Ti system, that a small amount of oxygen could stabilize some metal rich phases. However, samples deposited in different systems, with various cleaning conditions (HF last or followed by DI water rinse), and with or without TiN capping all showed a similar complexity before NiSi formation, even if the oxygen content is expected to be very different. Why should the results then be so different in the present films? We believe it to be a combination of thinner films and measurements performed far from equilibrium. Earlier experiments were usually performed with much thicker layers using lower temperature isothermal conditions. Here, the layers are thin and the sample are steadily ramped in temperature in a way that the metal rich phase region may barely last one minute. With very thin phases, growing rapidly, the sample remains in dynamic conditions that may deviate from true equilibrium [17]. It is also possible that the film thickness falls below the critical length where diffusion ceases to be rate controlling [17, 18]. In the current case, we believe that the grain size of the film could also at the source of the current observations. The Ni films deposited here show very small grain sizes (~12 nm). Considering the diffusion coefficients for pure Ni [19, 20], we find that there is more than 10 orders of magnitude ratio between volume and grain boundary diffusion at 400 °C. In bulk samples the diffusion will be relatively slow but as the film gets thinner and the grains smaller, diffusion will mainly occur through the grain boundaries and will drastically accelerate. Phases then form at much lower temperature and possibly in a different sequence as is observed in the current work. Since the diffusion coefficient in $Ni_{31}Si_{12}$ (at grain boundaries) is about 400 times larger than that of Ni_2Si at 400 ^oC (a ratio that increases for lower temperatures) [21, 22], one would expect this phase to form first. Note that the grain boundary diffusion is even faster in the $Ni_{31}Si_{12}$ than in pure Ni [21, 22] (about same ratio as for Ni_2Si). As the phase changes from Ni to $Ni_{31}Si_{12}$ and the diffusion rate increases, it seems reasonable to expect the grain size to expand. Since the grain boundary diffusion coefficient of Ni_2Si is smaller than that of $Ni_{31}Si_{12}$, the grain size might remain relatively constant through the

formation of other metal rich phases. This is what has been observed here. The formation of Ni_3Si_2 has also not been suggested before [23] but its appearance could also be related to grain dimensions and large variations in diffusion coefficients from volume to grain boundary diffusion (the diffusion data is not readily available for this phase).

The phase evolution for the n doped substrate follows the same phase sequence as for the p-doped substrates shown on Fig. 4a. The width of the temperature ranges over which the Ni_3Si_2 phase exists are similar for the two type of dopants the formation temperature is lower for the p-doped substrates. Surprisingly, in this case, the x-ray data shows that Ni_3Si_2 could be followed by the return of the Ni_2Si phase. This suggests that the dopants strongly influence the phase sequence and the kinetics of formation.

Recent work suggests that some epitaxial $NiSi_2$ forms early in the phase sequence and is consumed by Ni_2Si or NiSi [12]. In our work, $NiSi_2$ inverted pyramids were not observed at low temperature with XRD or TEM. We note however that the XRD detection only probe a very small portion of the possible grain orientations and that since the pyramids are epitaxial, we would not be in a geometry to detect them by x-ray diffraction. Also, our TEM analysis was performed on n-doped samples only and the p-doped substrates were shown to be more subject to the low temperature $NiSi_2$ formation [12]. Further TEM is needed for investigation of both the presence of $NiSi_2$ at low temperature and the possible return of Ni_2Si after Ni_3Si_2 formation for p-doped substrates.

Agglomeration

For the thin films presented here, we have shown that the temperature region over which the low resistivity NiSi phase is stable, is limited by the agglomeration of the film more than by the transformation to the high resistivity $NiSi_2$ phase. This is critical for microelectronics applications as it further limits the process window for NiSi implementation.

When the temperature ramp rate is varied (Fig. 8.), the variations in formation temperature for a given phase allows the determination of activation energy through Kissinger analysis [24]. These calculations are meaningful only when the formation mechanisms are well understood. The decrease in formation temperature with increasing ramp rate for $NiSi_2$ is a clear example of a situation where this type of analysis is not suitable as it would lead to a negative activation energy. The drop in formation temperature can simply be understood from the nucleation controlled nature of the NiSi-$NiSi_2$ phase formation. With a slower ramp rate, the film has more time to agglomerate before nucleation can occur. In an agglomerated film, the nucleation and growth can only proceed to the edge of a small agglomerated volume of NiSi. To form any significant volume of disilicide, most small agglomerated volumes need to transform which require at least one nucleation center per isolated island: a condition that can only occur at higher temperature. The situation however is reversed for the very high temperature ramp rates, where the film does not have the possibility to agglomerate before the first nuclei of $NiSi_2$ form. In this non agglomerated film, growth of $NiSi_2$ can then proceed through the full film at a much lower temperature.

CONCLUSIONS

We have shown that multiple metal rich phases are present in the Ni-Si system when reacting a thin Ni film with an underlying Si substrate. The phase sequence is as follows: Ni, $Ni_{31}Si_{12}$, Ni_2Si, Ni_3Si_2, NiSi and $NiSi_2$. The presence of Ni_3Si before the $Ni_{31}Si_{12}$, even if unlikely, can not be ruled out without further TEM investigations. Two metal rich phases, $Ni_{31}Si_{12}$ and Ni_3Si_2, were not observed earlier and we believe that their presence here is related to the smaller

thickness of the film and mainly the high density of grain boundaries which allows for accelerated diffusion and lower temperature phase formation. The formation temperatures for the metal rich phases highly depend on dopant type but are relatively insensitive to surface preparation. We also demonstrated that a serious limitation for NiSi implementation in devices is the low morphological stability of the film, which degrades before the monosilicide transforms to the high resistivity $NiSi_2$ phase. We find that the nucleation of $NiSi_2$ is very dependent on the temperature ramp rate as the morphological degradation of the film competes with the nucleation processes and retards the phase formation for low ramp rates.

ACKNOWLEDGMENTS

The authors would like to thank R.A. Carruthers for sample deposition. The synchrotron XRD experiments were conducted under DOE contract DE-AC02-76CH-00016. C. Detavernier is partly supported by the Nationaal Fonds voor WetenschappelijkOnderzoek- Vlaanderen.

REFERENCES

[1] C. Lavoie et al., *Defect and Diffusion Forum* **194-199** (2001) 1477.
[2] C. Lavoie et al., *J. Electr. Mat.*, in press for **31** (June 2002).
[3] G. B. Stephenson et al, *Rev. Sci. Instrum.* **60** (1989) 1537.
[4] C. Lavoie et al, *Mat. Res. Soc. Symp. Proc.* **406** (1996) 163-8.
[5] Handbook of Binary Alloy Phase Diagrams (CD version 1.0), ASM international, ISBN PC - 0-87170-562-1.
[6] M.-A. Nicolet and S. S. Lau, Formation and Characterization of Transition-Metal Silicides, in *VLSI Electronics: Microstructure Science, Vol.6,*(Academic Press, NY 1983), pp.330-464.
[7] J. M. Poate, K. N. Tu, J. W. Mayer, *Thin Films- Interdiffusion and Reactions* (Wiley NY 1978) p.337.
[8] J. M. Bennett and L. M. Mattson, *Introduction to Surface Roughness and Scattering* (Opt. Soc. Am., Washington, 1989).
[9] Joint Committee on Powder Diffraction Standard (JCPDS), ICDD, card # 17-0881, 14-0429.
[10] JCPDS card # 71-0638, 24-0524, 17-0222.
[11] JCPDS card # 73-2092, 48-1339, 03-0943.
[12] V. Teodorescu et al., *J. Appl. Phys.* **90** (2001)167.
[13] D. Turnbull, *J. Chem. Phys.* **20** (1952) 411.
[14] F. M. d'Heurle, *J. Mater. Res.* **3** (1988) 213.
[15] F. M. d'Heurle et al, *J. Appl. Phys.* **55**, 4208 (1984).
[16] *Properties of Metal Silicides*, ed. K. Maex and M. van Rossum, EMIS data reviews series #14, INSPEC (1995).
[17] F. M. d'Heurle, P. Gas, J. Philibert and O. Thomas, *Metals Materials and Processes* **11** (1999) 217.
[18] K. Barmak and J. M. Rickman, *Metals Materials and Processes* **11**, (1999) 177.
[19] H. Bakker, *Phys. Stat. Sol.* **28** (1968) 595.
[20] K. maier, H. Mehrer, E. Lessmann, W. Schule, *Phys. Stat. Sol. (b)* **78** (1979) 689.
[21] J. Gülpen, A.A. Kodentsov, F.J.J. van Loo, *Z. Metallk.* **86** (1995) 530.
[22] J. Gülpen, Ph.D. Thesis, Technical University of Eindhoven (1985).
[23] P.Gas, F.M. d'Heurle, F.K. Legoues, S.J. Laplaca, *J. Appl. Phys.* **59** (1986) 3458.
[24] P.G. Boswell, *J. Thermal Anal.* **18** (1980) 353.